Title

TALE-light imaging reveals maternally guided, H3K9me2/3-independent emergence of functional heterochromatin in Drosophila embryos

Journal

Genes & Development, 30(5)

ISSN

0890-9369

Authors

Yuan, Kai
O'Farrell, Patrick H

Publication Date

2016-03-01

DOI

10.1101/gad.272237.115

Peer reviewed

Submitted version

Final Published in Genes and Development (2016) 30, 579- 593, Cold Spring Harbor Press.

Live imaging reveals maternally-guided, H3K9me-independent emergence of functional heterochromatin in *Drosophila* embryos

Kai Yuan, Patrick H. O'Farrell
Department of Biochemistry, UCSF, San Francisco, CA

Department of Biochemistry, UCSF, S372C Genentech Hall, MB, 600 16th St.
San Francisco, CA 94158-2517

Running title: TALE-lights illuminate heterochromatin formation

Summary

Metazoans start embryogenesis with a relatively naïve genome. Formation of heterochromatin and progressive reinstallation of epigenetic marks underlie embryonic development and differentiation. Utilizing the recently developed TALE-lights method, we illuminated constitutive heterochromatin formation at the level of individual blocks of repetitive sequence in *Drosophila* early embryos. Certain repetitive sequences, including the 359-bp repeat, became heterochromatinized at the mid-blastula transition (MBT). Recruitment of HP1a, a hallmark of heterochromatin, to the 359-bp repeat was dependent on its C-terminal extension sequence but not its chromo-domain, and maternally provided signals guided this targeted accumulation of HP1a. HP1a-binding modulated replication-timing of individual repetitive sequences, as artificial recruitment of HP1a delayed replication whereas selective removal of HP1a advanced it. Our results reveal that "constitutive" heterochromatin emerges following a stereotyped developmental program in which different repetitive sequences are guided to the final heterochromatic state by diverse mechanisms, and thus generate new insights into the inheritance of heterochromatin.

Introduction

Among the earliest steps of metazoan embryogenesis is the epigenetic reprogramming after fertilization, which includes remodeling of nucleosomes, change of histone modification patterns, and DNA demethylation events (mostly studied in mammals). These active mechanisms, along with the passive dilution effect caused by the rampant early embryonic cell divisions, are thought to reset the newly formed zygotic genome to a relatively naïve state necessary for the regaining of totipotency (Fadloun et al., 2013; Farrell and O'Farrell, 2014). As the embryo continues developing, the epigenetic constraints are progressively restored and thus canalize the cells toward distinct cell fates. How the epigenetic regulations are re-established and transmitted during embryogenesis lies at the heart of this "canalization" process, but it remains poorly understood.

Selective silencing of the genome by heterochromatin formation is one of the most important epigenetic events (Beisel and Paro, 2011). In multicellular organisms, two types of

heterochromatin exist: constitutive heterochromatin and facultative heterochromatin. The former, characterized by enrichment of di- or tri-methylated H3K9 (H3K9me2/3) and HP1a, silences genomic regions enriched with tandem repeats of DNA motifs (aka satellite sequences) and remnants of transposable elements (TEs) (Elgin and Reuter, 2013). The latter, characterized by high levels of tri-methylated H3K27 (H3K27me3) and Polycomb proteins, represses developmental genes involved in cell fate determination (Simon and Kingston, 2013). In early embryos, most signatures of both types of heterochromatin are erased and have to be re-established *de novo*. How to deploy these powerful silencing systems accurately is a developmental challenge. Here, by focusing on the formation of the constitutive heterochromatin on different satellite sequences in *Drosophila* embryos, we start to unveil the molecular process of transmission and re-establishment of epigenetic regulations during embryogenesis.

Like many other organisms, *Drosophila* begins embryonic development with rapid cell divisions (Farrell and O'Farrell, 2014). Following the first gonomeric division, during which the male and female pronuclei meet, the zygotic nuclei undergo 7 mitotic divisions (cycles 2-8) that are perhaps the shortest cell cycles ever documented (8.6 minutes for every division), resulting in a shell of nuclei inside a shared cytoplasm--the syncytium. At cycle 9, this shell of nuclei migrates to the surface of the embryo and forms the blastoderm. The nuclei then continue dividing rapidly another 4 times (cycles 10-13), with progressively increased interphase durations from approximately 9 minutes in cycle 10 to 14 minutes in cycle 13. This commitment to the cell cycle quickly expands the number of zygotic nuclei. Many other cellular processes and developmental events are deferred until the slowing of the cell cycle at cycle 14. The interphase of cycle 14 is abruptly lengthened to 70 minutes or more depending on the spatial position of the cell in the embryo. In this lengthened interphase 14, cortical nuclei are cellularized, many maternal mRNAs and proteins degraded, and zygotic transcription fully activated. The embryonic development thus switches from maternal to zygotic program (Lee et al., 2014). This major embryonic transformation is called the mid-blastula transition (MBT).

Various satellite sequences in somatic cells are packaged into constitutive heterochromatin, which has unique attributes including high compaction, enrichment of H3K9me2/3 and HP1, transcriptional quiescence, and late replication. Most of these attributes are absent in the pre-blastoderm embryos, and the satellite sequences seem to take on these features successively as the embryo develops. Analysis of the C-banding patterns of the mitotic chromosomes (Vlassova et al., 1991), as well as assessment of the volume of a particular satellite sequence (Shermoen et al., 2010), suggests that satellite DNA becomes compacted prior to the blastoderm stage; while neither the establishment of H3K9 methylation in heterochromatic regions, nor the H3K4 methylation in euchromatic regions, was observed until interphase 14 (Rudolph et al., 2007). Using a heat shock-driven *lacZ* transgene inserted near satellite sequences, it was reported that the silencing activity of constitutive heterochromatin was first detectable in the gastrulating embryo, which is approximately in G2 of interphase 14 (Lu et al., 1998). In addition, BrdU or dUTP incorporation experiments revealed that satellite sequences became late-replicating in interphase 14 (Edgar and O'Farrell, 1990; Shermoen et al., 2010). These observations imply that constitutive heterochromatin is matured around the time of MBT. The early embryonic formation of constitutive heterochromatin seems to play a unique role in the establishment of the final nuclear architecture, as selective compromising HP1 function in early embryos by genetic manipulations influenced transcriptional silencing activity of heterochromatin in adults (Gu and Elgin, 2013).

One caveat of the studies described above is the lack of spatial resolution. Constitutive heterochromatin contains many compositionally different satellite sequences located at distinct genomic positions, and binding proteins specific to individual satellite sequences have been identified (Cortes and Azorin, 2000; Levinger and Varshavsky, 1982; Torok et al., 2000). Thus, without analyzing the behavior of each individual satellite sequence, our understanding on constitutive heterochromatin formation would be oversimplified. Here, by utilizing the recently developed TALE-lights method (Yuan et al., 2014), we characterized the formation of heterochromatin on satellite sequences in *Drosophila* early embryos at unprecedented spatial-temporal resolution. We observed, at the time of MBT, a stereotyped program of introduction of molecular markers of heterochromatin on some repetitive sequences (359-bp), but not on the others (1.686 and *dodeca*). The resultant change of local chromatin landscape altered the order of replication of those repeats. Moreover, we interrogated the molecular mechanism of heterochromatinization of the 359-bp repeat, and uncovered that signals from the mother guided the initial accumulation of HP1a at the 359-bp loci, independent of the histone mark H3K9me2/3. This study highlights the sophistication of the programs that introduce heterochromatic features to different regions of the genome within a nucleus, and generates new insight into the inheritance of constitutive heterochromatin.

Results

Establishment of repressive histone modifications at the mid-blastrula transition

Previously we observed that the replication of one satellite sequence, the 359-bp repeat, was only moderately delayed at the onset of late replication in interphase 14, but shifted to a much later time in interphase 15 (Figure 1A) (Shermoen et al., 2010; Yuan et al., 2014). We wanted to probe the mechanism of this selective sudden delay in replication, and reasoned that local epigenetic changes might be involved. DNA methylation is absent in *D. melanogaster* early embryos (Zemach et al., 2010), and histone modifications play a key role in early embryonic epigenetic reprogramming. We thus analyzed the methylation status on two key residues of histone 3, H3K9 and H3K27, which characterize constitutive heterochromatin and facultative heterochromatin respectively.

While there was almost no detectable immunostaining in pre-MBT embryos with antibodies targeting H3K9me2 or H3K9me3, stainings for both H3K9me2 and H3K9me3 emerged incrementally and with similar kinetics, accumulating in interphase 14 nuclei at the apical pole where the pericentric sequences surround the clustered centromeres (Figures 1B and 1C). Acetylation of H3K9 (H3K9ac), which is exclusive of H3K9me2/3 and marks euchromatin on chromosome arms, was also undetected in the early embryo but appeared in interphase 13, about one cycle earlier than the appearance of the methylated H3K9 (Figure S1A). Interestingly, staining for histone acetylation of H3K27 (H3K27ac), as well as histone H4 (H4ac), was readily detectable as early as in the pre-blastoderm embryos (Figures S1B and S1C); but its level decreased slightly in mid-late interphase 14 when the tri-methylated H3K27 (H3K27me3) started to appear (Figure 1D).

In summary (Figure 1E), during the early embryonic development, histone acetylation appears early, accompanying the rampant DNA replication and the gradual activation of the zygotic genome (Li et al., 2014). On the other hand, the repressive histone modifications, H3K9me2/3 and H3K27me3, do not emerge until the much prolonged interphase 14, suggesting that the slowing of cell cycle at the MBT provides the first permissive situation for the establishment of repressive histone modifications.

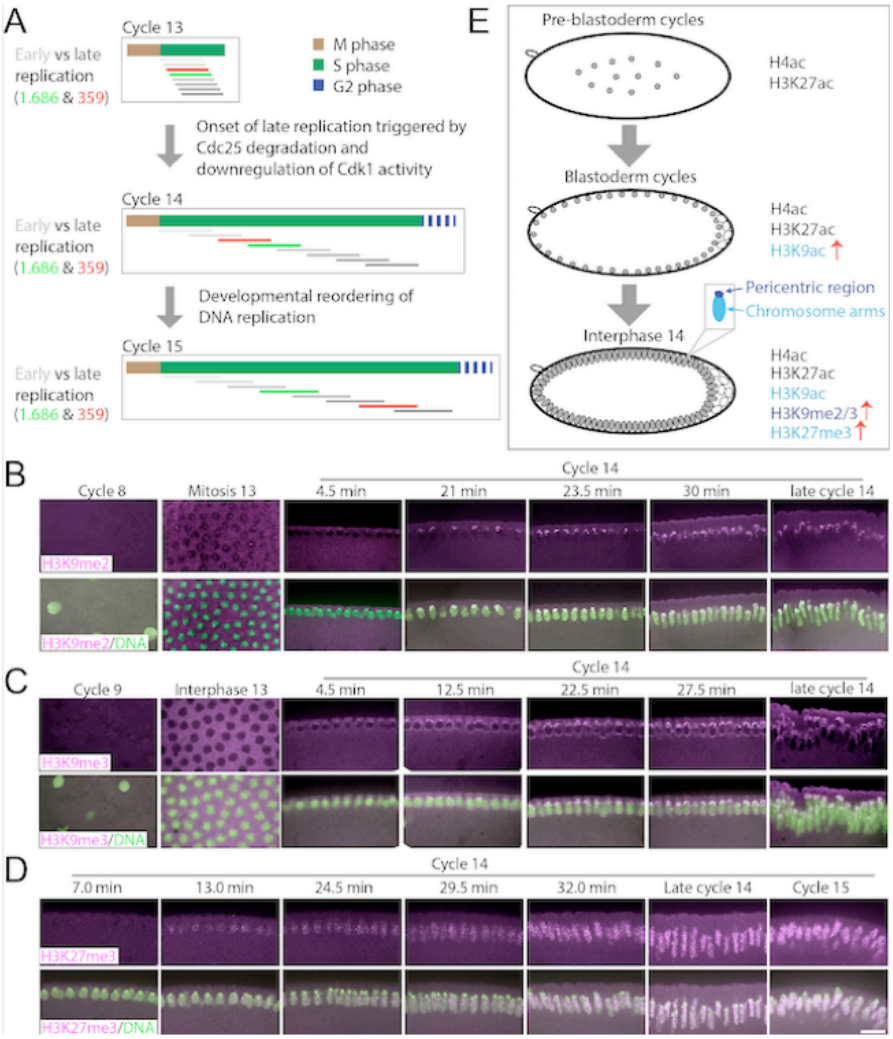

Figure 1 Onset of repressive histone modifications in interphase 14.
(A) Approximations show replication timing of early (light grey bars) and late-replicating (dark grey bars) sequences in the interphases around the MBT. Green and red bars represent the replication timing of two particular repetitive sequences, 1.686 and 359-bp, respectively. Note that after the global onset of late replication in cycle 14, these two repeats switch order in replication in cycle 15, due to the much-delayed replication of the 359-bp repeat.
(B-D) The emergence of methylated H3K9 (B and C) or H3K27 (D) in *D. melanogaster* early embryos. The antibody stainings are shown in magenta and Picogreen-stained DNA in green. The estimated developmental time, determined either by inter-nuclear distance for embryos in the syncytial blastoderm stage or by the length of the nuclei for embryos in cycle 14, is marked at the top. Scale bar, 10 μm.
(E) A graphic summary of histone modification patterns in *D. melanogaster* early embryos. In addition to the difference in their temporal appearance, different histone modifications show distinct spatial distribution. H3K9me2/3 is concentrated at the pericentric regions, whereas H3K9ac and H3K27me3 are along the chromosome arms.

Different repetitive sequences acquire distinct chromatin features at the MBT

Various highly repetitive sequences that occupy over 20% of the *D. melanogaster* genome are almost always heterochromatic and comprise "constitutive heterochromatin" (Wei et al., 2014). The appearance of H3K9me2/3 in interphase 14 marks a step in embryonic formation of constitutive heterochromatin. To probe whether each type of repeat sequence responds similarly to the developmental cues, we analyzed the emergence of histone modifications at sub-heterochromatic level, on different satellite sequences.

We have previously developed protein probes called TALE-lights that can be programmed to recognize a given DNA sequence (Figure 2A). Injection of a TALE-light at an optimal concentration highlighted particular satellite sequences live without disrupting embryogenesis (Movie S1). Similarly, staining of fixed embryos with the TALE-light lit up the target sequences (Figure S2A). The dynamics of the mitotic chromosome seemed to affect the TALE-light's recognition of its target, as the TALE-light signal went down during mitosis in live embryos but not in fixed samples (Figure S2B).

We made TALE-lights that recognize two major satellite sequences in *D. melanogaster* genome, 359-bp and 1.686 (Yuan et al., 2014). Co-staining of the TALE-light and anti-histone 3 antibody suggested that these repetitive regions contained nucleosomes in the early embryo (Figures S2C-S2D),

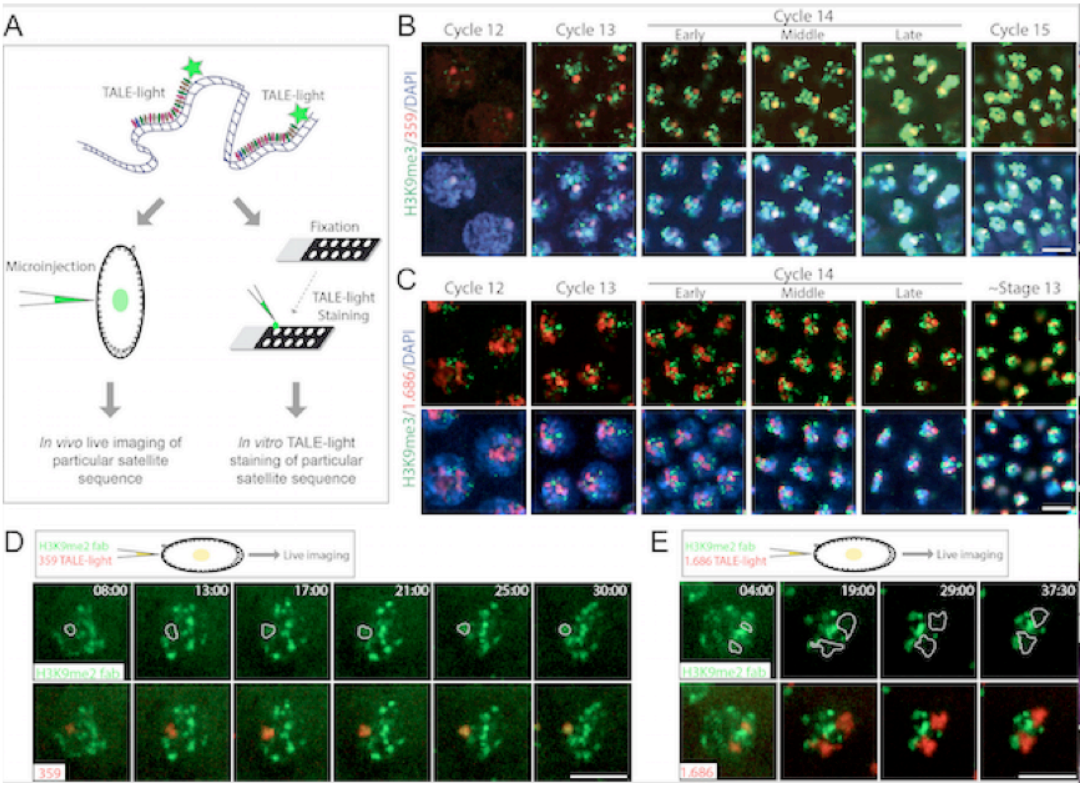

Figure 2 Differential accumulation of methylated H3K9 on the 1.686 and 359-bp repeats.
(A) Schematic of the *in vivo* and *in vitro* applications of the TALE-lights.
(B-C) The appearance of H3K9me3 mark on the 359-bp (B) and 1.686 (C) repetitive sequences during embryogenesis. Antibody staining of H3K9me3 is shown in green, TALE-lights staining of the 359-bp or 1.686 repeat in red, and DAPI-stained DNA in blue. Note that panel C includes an embryo at stage 13, which is at the end of germ band retraction (560-620 min after fertilization). Scale bars: 5 μm.
(D-E) *In vivo* visualization of accumulation of H3K9me2 mark on particular repetitive sequences by combining the TALE-light imaging with the FabLEM technique. Time-lapse images of nuclei in the injected interphase 14 embryos are shown. The reformation of the interphase nucleus is set to be 00:00 (min:s). Fab fragment recognizing the H3K9me2 mark is shown in green, and TALE-lights in red. The dotted circles in the upper panels outline the TALE-lights labeled regions. Scale bars: 5 μm.

although the AT-rich 1.686 region seemed to either be less compact or have lower nucleosome occupancy (Krassovsky and Henikoff, 2014) when compared with adjacent regions (Figure S2D). Those early embryos showed little or no staining for most of the histone modifications tested in these two repetitive regions (Figures S2E-S2F, S2I-S2L), except for trace staining of acetylated H3K27 and H4 at the 359-bp loci early on (Figures S2G and S2H). In interphase 14, methylated H3K9 started to emerge on the 359-bp repetitive sequences, and it was maintained in the following cell cycles (Figure 2B). Meanwhile, no H3K9 methylation was observed in the 1.686 region. The methylated H3K9 in the 1.686 region emerged much later in embryogenesis and in a more sporadic manner (Figure 2C, ~stage 13).

A Fab-based live endogenous modification labeling (FabLEM) technique has been developed to visualize histone modifications in vivo (Stasevich et al., 2014). To confirm the differential emergence of H3K9 methylation at 359-bp and 1.686 loci in developing embryos, we injected the TALE-light to visualize the corresponding satellite sequences and a FabLEM probe to label H3K9me2. In agreement with the TALE-light staining results, the 359-bp region, but not the 1.686 region, gradually recruited the H3K9me2 probe in interphase 14 (Figures 2D and 2E). We conclude that the onset of significant

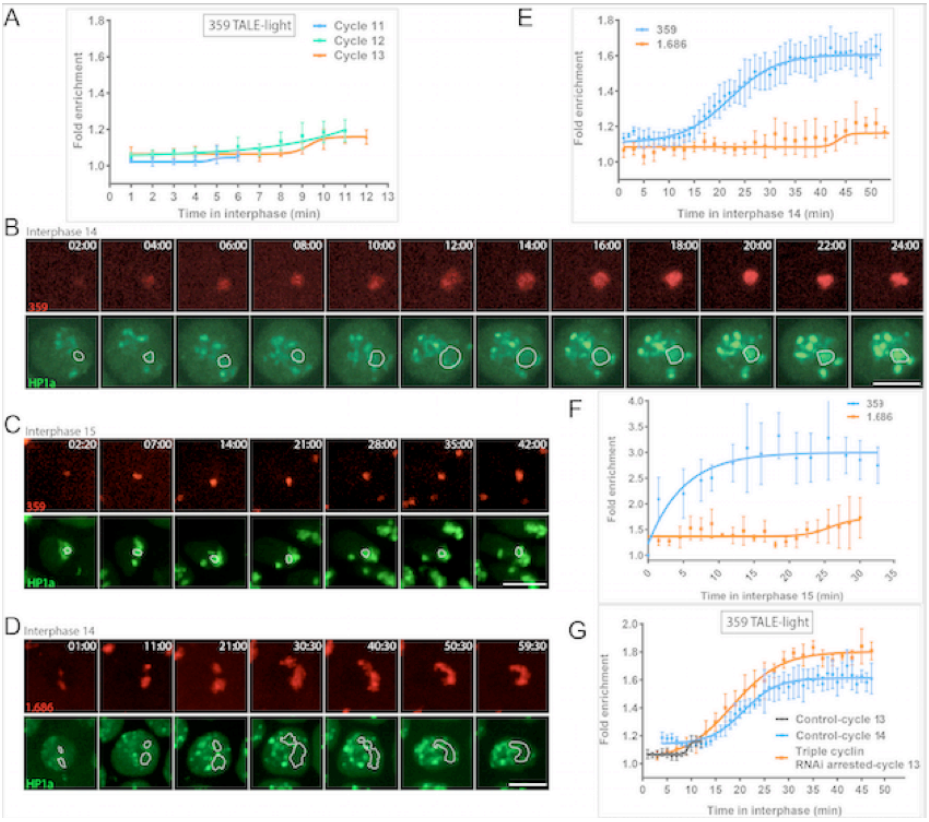

Figure 3 Developmentally regulated heterochromatin formation on the 359-bp repeat.
(A) Quantification of GFP-HP1a accumulation at the 359-bp loci from interphase 11 to 13 (method detailed in Figure S3C and Experimental procedure, n>3, error bars represent the SD).
(B-C) Frames from videos at the indicated times (min:s) show GFP-HP1a accumulation at the 359-bp loci (dotted circle) in interphase 14 (B) and interphase 15 (C). Note that in interphase 15 GFP-HP1a is rapidly recruited to the 359-bp region after mitosis. The reappearance of interphase nucleus is set to be 00:00. Scale bars: 5 μm.
(D) Time-lapse images show no obvious accumulation of GFP-HP1a at the 1.686 loci in interphase 14. Scale bar: 5 μm.
(E-F) Quantification of GFP-HP1a accumulation at the 359-bp (blue curve) and 1.686 (orange curve) loci in interphase 14 (E) and interphase 15 (F). Error bars represent the SD (n>3).
(G) GFP-HP1a accumulation at the 359-bp loci in triple cyclin RNAi-arrested interphase 13 embryos (orange curve) is comparable to that in the control interphase 14 embryos (blue curve). GFP-HP1a accumulation in control interphase 13 is also shown for comparison (grey curve). Error bars represent the SD (n>3).

accumulation of H3K9me2/3 is delayed until cycle 14, and that it accumulates progressively following distinct time courses at different loci.

Developmental regulation of heterochromatin formation on the 359-bp repeat

The differential accumulation of H3K9me2/3 during cycle 14 suggests heterochromatin formation on the 359-bp repeat but not on the 1.686. It is thought that H3K9me2/3 binds and recruits HP1a, and the establishment of a stable HP1a-bound state underlies or at least marks the molecular process of heterochromatin formation.

To characterize how the 359-bp repeat is heterochromatinized, we made recombinant HP1a protein with a GFP tag fused to its N-termini (Figure S3A). We injected the GFP-HP1a along with the TALE-light probe to visualize heterochromatin formation on particular satellite sequences in developing embryos. Western-blot analysis showed that the injected exogenous GFP-HP1a was at a comparable concentration with the endogenous HP1a (Figure S3B).

At each mitosis, the TALE-light probe targeting the 359-bp repeat was displaced from mitotic chromosomes but soon re-accumulated to the 359-bp loci as the nuclei exited mitosis. We followed the accumulation of GFP-HP1a within the TALE-light labeled region in each interphase during early embryogenesis (e.g. Figure 3B, lower panels, dotted cycle), and quantified the enrichment of GFP-HP1a at the 359-bp loci by

calculating the fold enrichment over a control area in the same nucleus (Figure S3C and Experimental Procedure). From interphase 11 to interphase 13, GFP-HP1a was enriched at several discrete loci in the nucleus; but little was found in the 359-bp region (Figure 3A, Movie S2), which was consistent with the observation that H3K9me2/3 was absent at this stage. Dramatic accumulation of GFP-HP1a at the 359-bp loci was observed in interphase 14 (Figure 3B, Movie S3). After a rapid accumulation phase from 15 min to 30 min into interphase 14, the amount of GFP-HP1 within the 359-bp region reached a plateau (Figure 3E, blue curve). This HP1a-bound state of the 359-bp repeat was stably maintained thereafter (Figure 3F, blue curve). As shown in Figure 3C, in interphase 15, the 359-bp loci was decorated by GFP-HP1a right after the mitotic exit and became part of the chromocenter.

It was noteworthy that we observed a small amount of GFP-HP1a within the 359-bp region at the end of interphase 13 and even interphase 12 (Figure 3A, Movie S2), suggesting that the 359-bp repeat attempted to recruit HP1a but the rapid cell divisions interrupted this process. To test this, we knocked down all the three mitotic cyclins by RNAi to arrest the embryos in interphase 13 (Farrell et al., 2012), and analyzed the accumulation of GFP-HP1a at the 359-bp loci. Indeed, stopping the rapid cell cycle allowed early recruitment of GFP-HP1a to the 359-bp loci (Figure 3G, orange curve). This result further supported the idea that interphase extension at the MBT was a prerequisite for the formation of heterochromatin at the 359-bp loci.

The 1.686 repeat, on the contrary, didn't recruit GFP-HP1a (Figures 3D-3F), echoing the lack of H3K9me2/3 mark in the 1.686 region at this stage. Together, our results reveal clear distinctions in the process of heterochromatin formation between different repetitive sequences. As building blocks of the constitutive heterochromatin, it is apparent that different repetitive sequences take different routes to reach the heterochromatic state during embryogenesis.

Ordering the events during heterochromatinization

The heterochromatinization of the 359-bp repeat in interphase 14 provides an opportunity to dissect the underlying molecular mechanism. It is known that H3K9me2/3 helps recruit HP1a, and HP1a promotes the spreading of the H3K9me2/3 mark by recruiting histone methyltransferase (Canzio et al., 2014). We thus tested what initiates the heterochromatinization process on the 359-bp repeat.

The N-terminal chromodomain (CD) of HP1a specifically recognizes the H3K9me2/3 mark, whereas the C-terminal chromoshadow domain (CSD) dimerizes and forms an interface that recruits proteins containing the PxVxL motif, where x is any amino acid (Figures S4B and S4C). A single amino acid substitution in CD (V26M) abolishes the recognition of H3K9me2/3, and a substitution W200A in the C-terminal extension sequence disrupts the binding of PxVxL motif without affecting HP1a's dimerization (Canzio et al., 2014). The V26M and W200A double mutant lost all the specific localization in interphase nuclei (Figure 4A and S4A), suggesting that one or the other targeted sites are required for HP1a binding at this developmental stage. Interestingly, restoration of a functional CD and hence the H3K9me2/3 binding activity (HP1a-W200A) brought back a subset of the HP1a foci but didn't rescue the timely accumulation at the 359-bp locus (Movie S5). It was only faintly enriched within the 359-bp region toward the end of interphase 14 (Figure 4B), and quantification analysis showed that it lacked the rapid accumulation phase seen with the wild type (Figure 4E). In contrast, the HP1a-V26M, which is capable of binding to the PxVxL motif but not the H3K9me2/3 mark, was efficiently recruited to the 359-bp loci (Figure 4C, Movie S4), although the quantification analysis indicated that its accumulation curve plateaued at a reduced height (Figure 4E), which might imply

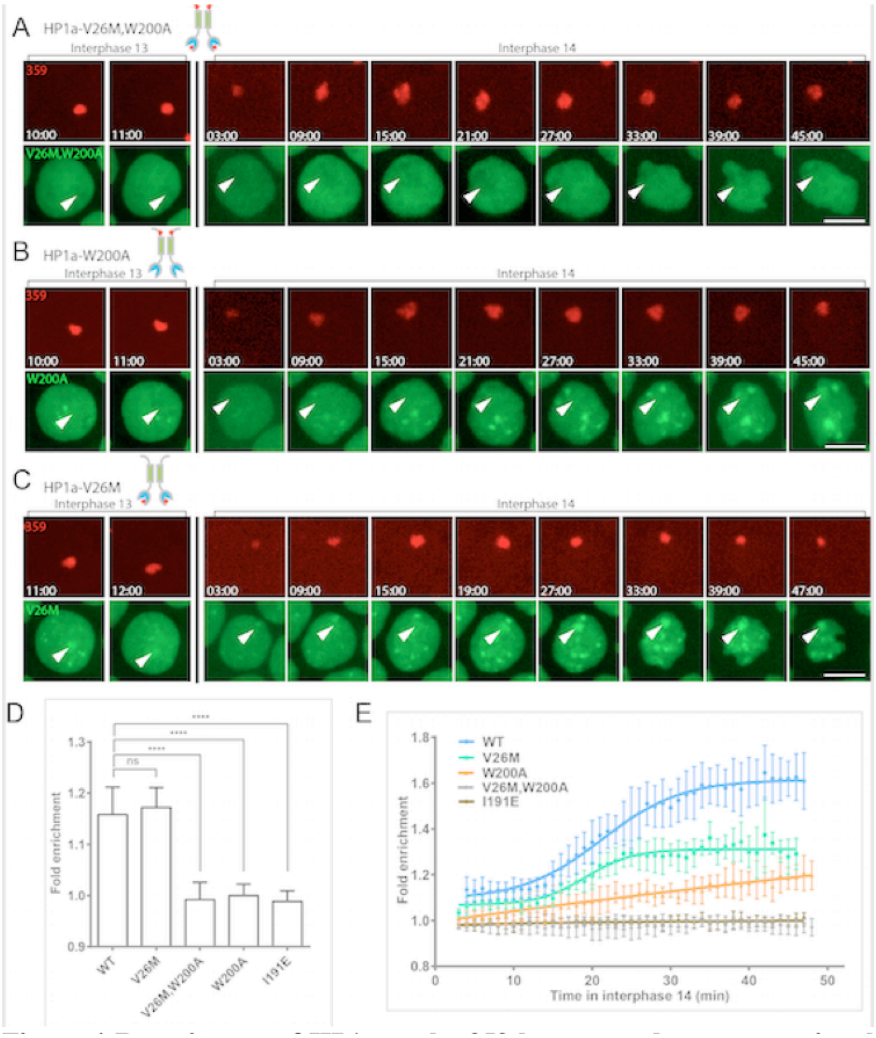

Figure 4 Recruitment of HP1a to the 359-bp repeat does not require the chromo-domain.
(A-C) Time-lapse images show accumulation of the indicated GFP-HP1a mutant on the 359-bp repeat at the end of interphase 13 (first two columns) or during interphase 14 (the rest of the columns). Note that the reformation of nucleus in each interphase is set to be 00:00 (min:s). Red stars in the schematic of HP1a structure indicate the position of the point mutations. Arrowheads in the green panels point to the corresponding 359-bp loci. Scale bars: 5 μm.
(D) Enrichment of the indicated GFP-HP1a protein within the 359-bp region at the end of interphase 13. The V26M mutant is enriched at the 359-bp loci similar to the wild type HP1a (unpaired t test, $p=0.5546$), whereas the W200A, V26M/W200A, and I191E mutants are not enriched (unpaired t test, $p<0.0001$). Error bars represent the SD.
(E) Quantification of different GFP-HP1a mutants accumulating at the 359-bp loci in interphase 14. Error bars represent the SD ($n>5$).

that a deficiency in H3K9me2/3 recognition compromises the late accumulation phase of HP1a. Together, these results suggested that the initial recruitment of HP1a to the 359-bp repeat did not depend on the capability to bind the H3K9me2/3 mark, but required an ability to interact with proteins that contain the PxVxL motif. Consistent with this, the HP1a-I191E mutant that cannot dimerize and hence loses the ability to bind the PxVxL ligand, also failed to accumulate on the 359-bp repeat (Figure S4D).

A small amount of GFP-HP1a could be seen in the 359-bp region at the end of interphase 13 (Figures S4A and 4C, first two columns). We further quantified and compared this premature recruitment among different HP1a mutants. As shown in Figure 4D, no significant reduction was observed for HP1a-V26M when compared with the wild type; mutants without the ability to bind the PxVxL motif however, failed to be recruited at this stage. Thus, we conclude that the initial recruitment of HP1a to the 359-bp region does not depend on binding to H3K9me2/3. This is consistent with the late and gradual accumulation of this methyl mark described above.

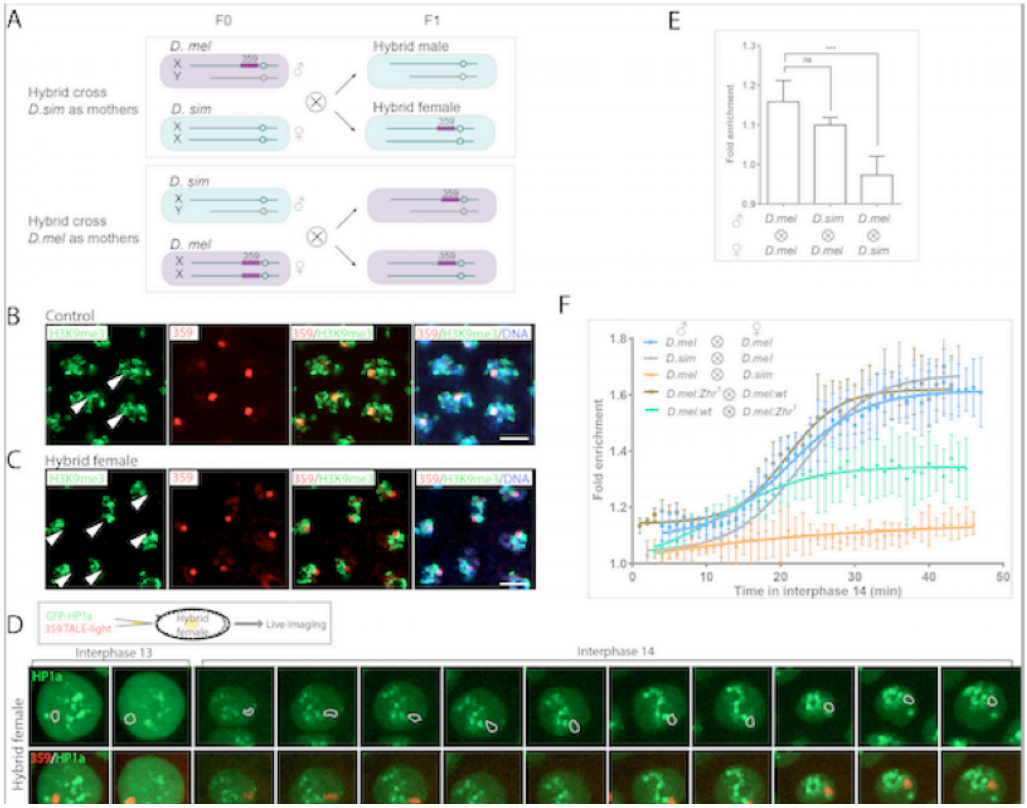

Figure 5 Maternal cue guides heterochromatinization of the 359-bp repeat.
(A) Schematic of the hybrid cross between *D. simulans* and *D. melanogaster*. Only sex chromosomes are shown. Note that the 359-bp repeat located on the X chromosomes of *D. melanogaster* is absent in *D. simulans*.
(B-C) TALE-lights and H3K9me3 antibody stainings in the control and the hybrid female embryos produced from the *D. simulans* and *D.melanogaster* cross. H3K9me3 histone mark exists within the 359-bp region in control (B) but not in the hybrid female embryos (C, arrowheads). H3K9me3 is shown in green, the 359-bp repeat in red, and DNA in blue. Scale bars: 5 μm.
(D) Frames from videos at the indicated times (min:s) show a lack of GFP-HP1a accumulation on the 359-bp repeat (dotted circle) in the hybrid female embryos. Note that the reappearance of nucleus in each interphase is set to be 00:00. Scale bar: 5 μm.
(E) Enrichment of GFP-HP1a within the 359-bp region at the end of interphase 13 in 359-bp repeat-bearing embryos produced from the indicated crosses. No significant difference is observed in embryos laid by *D. melanogaster* mothers (unpaired t test, p=0.0653); however embryos from the *D. simulans* mothers have less GFP-HP1a at the 359-bp loci when compared with control (unpaired t test, p=0.0002). Error bars represent the SD.
(F) Quantification of GFP-HP1a accumulation in interphase 14 at the 359-bp loci in the 359-bp positive embryos produced from the indicated crosses. Error bars represent the SD (n>5).

Nuclear position is not a major determinant of heterochromatin formation on the 359-bp repeat

We wanted to know what signal guided the HP1a accumulation on the 359-bp repeat. Constitutive heterochromatin is spatially separated from euchromatin in the nucleus of most somatic cells, and it is often positioned adjacent to the nuclear lamina and the periphery of the nucleoli (Padeken and Heun, 2014). The unique nuclear position has been suggested to play a role during the establishment of heterochromatin (Jachowicz et al., 2013). We assessed the functional input of nuclear position during the heterochromatinization of the 359-bp repeat.

The majority of the 359-bp repeat localizes on the proximal end of the X chromosome. In the scute 8 mutant, which is associated with a major inversion on the X chromosome with an end point within the proximal part of the 359-bp repeat, most of the 359-bp repetitive sequences are translocated to the distal end of the X chromosome with a small block of the 359-bp repeat remaining at its original centromere proximal position (Figures S5C and S5D).

We characterized the GFP-HP1a accumulation at the large, more telomeric block of the 359-bp

repeat, which is positioned at the basal pole of the nuclei (Figure S5E), as well as the smaller, more centromeric block of repeat that is positioned apically (Figure S5F). GFP-HP1a was recruited to both loci of the 359-bp repeat simultaneously in interphase 14, suggesting that nuclear position at this stage is not a major contributor to the formation of heterochromatin. Quantification indicated that the accumulation of GFP-HP1a to the basal 359-bp locus plateaued at a reduced height (Figure S5G), which might be partially due to the measurement inaccuracies during live embryo imaging caused by the elongating nuclei in interphase 14 (Waters, 2009), which pushed the basal 359-bp locus up to 14 μm away from the coverslip.

Maternal cues guide heterochromatin formation

A widespread feature of early embryogenesis is that the mother preloads the egg with material that directs most of the early developmental programs (Farrell and O'Farrell, 2014). We reasoned that maternal signals might guide the heterochromatin formation on the 359-bp repeat. To test this, we removed the 359-bp repeat from the mother's genome and evaluated the heterochromatinization of the 359-bp repeat in the offspring embryos.

Repetitive sequences evolve rapidly. Another closely related species, *D. simulans*, has no 359-bp or 359-bp like repeat in its genome and can be crossed to *D. melanogaster* (Ferree and Barbash, 2009). As illustrated in Figure 5A, when female *D. simulans* was husbanded with male *D. melanogaster*, the F1 hybrid female embryos would have the maternal supply from the *D. simulans* mother that lacks the 359-bp repeat, and meanwhile obtain a copy of the 359-bp repeat from the *D. melanogaster* father. Most of these hybrid female embryos were early embryonic lethal, due to chromosome mis-segregation in the syncytial cycles (Figures S5A and S5B). However, a small fraction developed to a later embryonic stage beyond the MBT. We analyzed the H3K9 methylation in these embryos. While H3K9me3 was found on the 359-bp repeat in control interphase 14 embryos (Figure 5B, arrowheads), it was absent in the hybrid female embryos (Figure 5C, arrowheads). Consistently, in these embryos the HP1a accumulation at the 359-bp loci was greatly reduced when compared with that in the control or the embryos from the reciprocal cross (Figures 5D and 5F, Movie S6). The initial recruitment of HP1a at the end of the interphase 13 was also compromised in these embryos. In the reciprocal cross in which *D. melanogaster* was the mother, embryos exhibited early recruitment of HP1a, whereas embryos from the *D. simulans* mother failed to do so (Figure 5E).

The cross species mating suggests that the maternal signal might depend on maternal presence of the 359-bp repeat. We wanted to test this with *D. melanogaster* strains. Besides a major block of 359-bp repeat on the X chromosome, *D. melanogaster* has many tiny 359-bp derivatives on its autosomes (Wei et al., 2014). The Zhr^1 mutant lacks the majority of the 359-bp repeat due to compound X chromosomes (Ferree and Barbash, 2009). We mated the Zhr^1 females with control males, and analyzed HP1a accumulation in the offspring female embryos. The removal of most of the 359-bp repeat from the maternal genome had a quantitative effect, as the accumulation of HP1a in interphase 14 at the 359-bp loci was significantly reduced in the offspring embryos when compared with that in the control or the embryos from the reciprocal cross (Figure 5F, Movie S7).

We conclude that maternally provided factors contribute to the heterochromatinization of the 359-bp repeat. This maternal contribution appears to depend on the maternal presence of the 359-bp sequences. Deficits of maternal 359-bp sequences specifically affect the 359-bp locus in the progeny embryos.

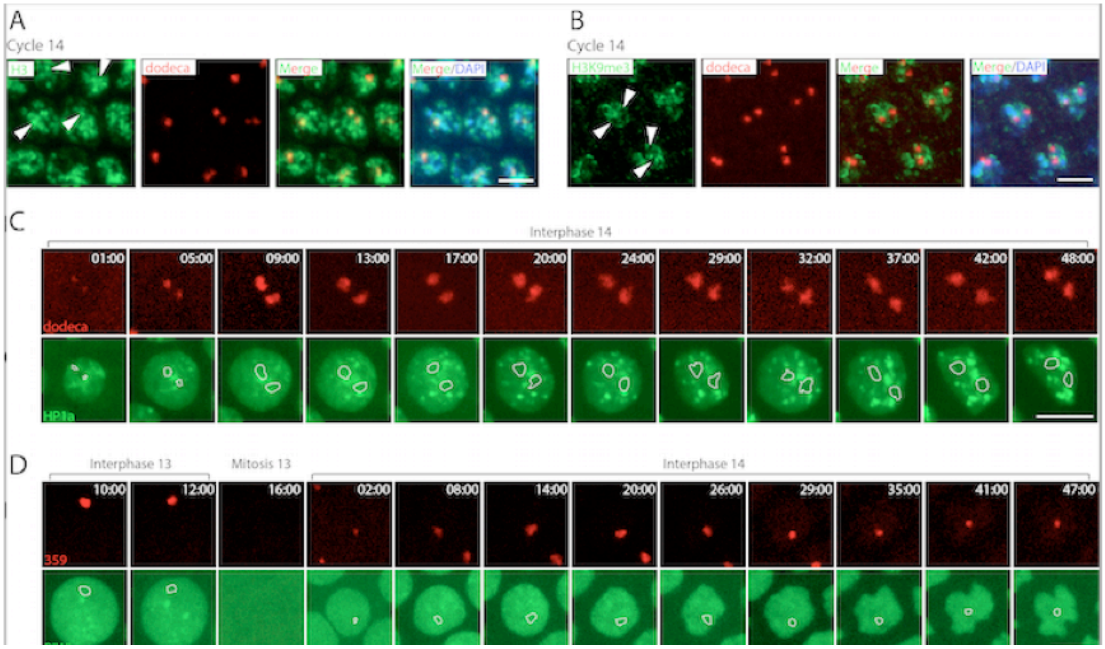

Figure 6 Another repetitive sequence, *dodeca*, is not heterochromatinized in interphase 14.
(A-B) Co-staining of the TALE-light targeting *dodeca* and antibody recognizing histone 3 (A) or H3K9me3 (B) show that histone 3 exists within the *dodeca* region but it lacks H3K9me3 modification. Antibody staining is shown in green, *dodeca* repeat in red, and DNA in blue. Scale bars: 5 μm.
(C) Time-lapse images (min:s) show that GFP-HP1a is not recruited to the *dodeca* loci (dotted circle) in interphase 14. Scale bar: 5 μm.
(D) Frames from videos at the indicated times (min:s) show that Piwi is not enriched at the heterochromatinizing 359-bp loci (dotted circle) in interphases 13 and 14. Note that the reformation of nucleus in each interphase is set to be 00:00. Both the 359-bp TALE-light and Piwi are dispersed into the cytoplasm during mitosis. Scale bar: 5 μm.

Possible involvement of small RNA in transgenerational inheritance of constitutive heterochromatin

Our results show that the initiation of heterochromatinization of the 359-bp repeat is independent of the recognition of H3K9me2/3 mark but requires maternal signals. We wanted to probe the nature of the maternal signal. One attractive candidate was the RNA species generated from the 359-bp repeat during oogenesis.

The previous analysis of small RNA profiles in early embryos showed the presence of both sense and antisense small RNAs originated from the 359-bp repeat or its derivatives 356-bp repeat (Chung et al., 2008; He et al., 2012), whereas the 1.686 repeat, which didn't undergo heterochromatinization in interphase 14, seemed to lack the corresponding small RNAs (Figure S6A). Interestingly, *dodeca*, another major repetitive sequence on the third chromosome, also didn't have its representative small RNAs in the early embryos. We made a TALE-light probe targeting the *dodeca* sequence, and followed its behavior in interphase 14. As shown in Figure 6C, GFP-HP1a didn't accumulate at the *dodeca* loci. Consistently, the TALE-light staining showed that the nucleosomes within the *dodeca* region lacked the H3K9me3 mark at this stage (Figures 6A and 6B).

Thus, the presence of small RNAs in the early embryo seems to correlate with heterochromatin formation on a certain repetitive sequence in interphase 14 (Figure S6A). However, Piwi-the potential candidate protein that links small RNAs and HP1a (Brower-Toland et al., 2007)-didn't show significant colocalization with either HP1a (Figure S6B) or the 359-bp TALE-light (Figure 6D, see discussion). Whether small RNAs are directly involved in the heterochromatin formation in fly early embryos and how they function are questions that still need to be addressed.

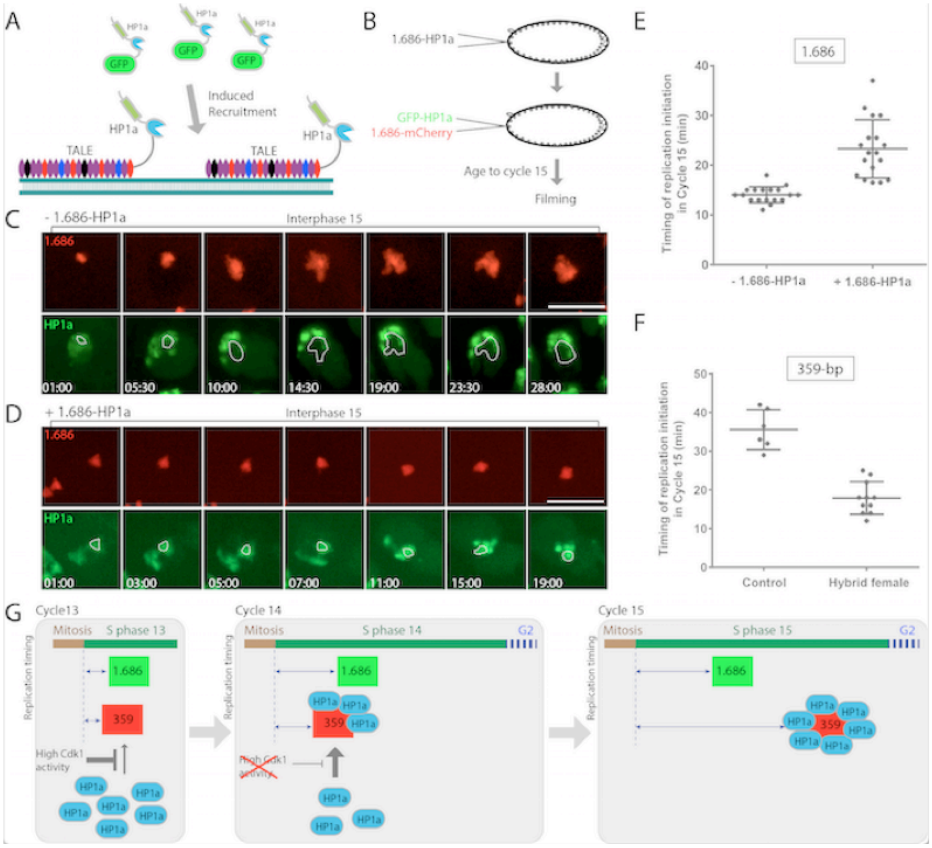

Figure 7 Establishment of the HP1a-bound state delays timing of replication in S phase.
(A) A cartoon depicting the induced accumulation of GFP-HP1a by the TALE-HP1a fusion protein.
(B) Schematic of the experiment showing the order of the injections.
(C-D) Time-lapse images show that GFP-HP1a is absent at the 1.686 locus in control interphase 15 embryos (C) but is recruited to the 1.686 region when 1.686-HP1a fusion protein is present (D). The reformation of the interphase 15 nucleus is set to be 00:00 (min:s). Scale bars: 5 μm.
(E) Replication timing of the 1.686 repetitive sequence in interphase 15 with or without the injection of the 1.686-HP1a fusion protein. The induced HP1a accumulation on 1.686 significantly delays its timing of replication (unpaired t test, $p<0.0001$). Error bars represent the SD.
(F) Replication timing of the 359-bp repeat in interphase 15. The 359-bp repeat in the hybrid female embryos from the *D. simulans* and *D.melanogaster* hybrid cross don't recruit HP1a, and its timing of replication in interphase 15 is significantly earlier than that in the control embryos (unpaired t test, $p<0.0001$). Error bars represent the SD.
(G) A graphic summary depicting HP1a accumulation on the 359-bp repeat around the time of MBT, and its influence on the replication timing.

Establishment of stable HP1a-binding delays timing of replication in S phase

The observed selective heterochromatinization of the 359-bp repeat in interphase 14 could potentially explain the previously reported sudden delay in replication timing of this repeat in interphase 15 (Yuan et al., 2014). To directly test whether the establishment of the HP1a-bound state delays replication, we induced HP1a accumulation on the 1.686 repeat and measured its timing of replication. Artificial tethering HP1a to DNA has been shown to induce local heterochromatin formation (Hathaway et al., 2012). We fused HP1a to the C-terminal of the TALE-light probe recognizing the 1.686 repeat, and injected this 1.686-HP1a fusion protein into the embryo to induce ectopic heterochromatin formation (Figures 7A and 7B). The targeted HP1a fusion protein induced robust accumulation of untargeted GFP-HP1a at the 1.686 loci in interphase 15 (Figure 7D). Moreover, the replication-coupled decompaction of the 1.686 loci seen in the control embryos was postponed (Figures 7C and 7D), indicating a delay in replication. We injected GFP-PCNA to directly visualize the bulk replication of the 1.686 repeat and compared its timing in embryos with or without the 1.686-HP1a. Indeed the presence of the 1.686-HP1a fusion protein delayed the replication of the 1.686 in interphase 15 (Figures 7E and S7A).

To examine the consequence of loss of HP1a recruitment, we used the GFP-PCNA reporter to follow replication timing of the 359-bp repeat in the *D. simulans* and *D. melanogaster* hybrid embryos in which the 359-bp repeat failed to recruit HP1a. The replication of the 359-bp loci was advanced when compared with that in the control embryos (Figures 7F and S7B). These two sets of experiment provided direct evidence for the idea that heterochromatin formation delays the local timing of replication in S phase. We thus conclude that the sudden delay of replication timing of the 359-bp repeat in interphase 15 is due to the developmentally regulated heterochromatinization of this repeat.

As summarized in Figure 7G, during the syncytial blastoderm stage, high Cdk1 activity and/or the rapid cell cycle inhibit the accumulation of the HP1a at the 359-bp loci. At the MBT in interphase 14, downregulation of the Cdk1 (Farrell and O'Farrell, 2014) and other developmental inputs (Blythe and Wieschaus, 2015) slow DNA replication and extend interphase, allowing the HP1a accumulation and hence heterochromatin formation on the 359-bp repeat. This local change in chromatin landscape impacts the DNA replication schedule in the following cell cycles, as the heterochromatic state of the 359-bp repeat selectively delays its timing of replication in relative to the other repeats.

Discussion

TALE-lights: visualizing specific DNA sequences in vivo and in vitro

New tools are needed to probe the complex and dynamic nature of the organization of the eukaryotic genome. For over 30 years, FISH has been the dominant method to label a given DNA sequence (Levsky and Singer, 2003), but the requirement of denaturation of DNA often compromises the integrity of the sample and hinders its applications in living organisms. The integration of the *lacO* or *TetO* repeats into a particular genomic locus and the use of fluorescently labeled LacI or TetR protein provide strategies to visualize DNA targets live (Robinett et al., 1996). However, these methods lack the flexibility in target selection. Recent breakthroughs have allowed the systematic engineering of DNA sequence recognition, which stimulated the development of several new DNA visualization methods, including techniques based on the zinc fingers (ZFs) (Lindhout et al., 2007), the CRISPR/dCas9 (Anton et al., 2014; Chen et al., 2013), and the transcription activator-like effectors (TALEs) (Ma et al., 2013; Miyanari et al., 2013; Thanisch et al., 2014; Yuan et al., 2014). Our TALE-lights belong to the last.

The sequence-specific DNA recognition by a TALE-light comes from the one-to-one binding of the TALE modules to each of the DNA bases. Therefore, its programmability is as flexible as the CRISPR/dCas9 and better than the ZFs, as one zinc finger domain recognizes a 3-bp 5'-GNN-3' DNA sequence (Segal et al., 1999). Moreover, our results demonstrated that the TALE-lights work well in both fixed and live conditions. Because of this unique feature, we believe that the TALE-lights will be a valuable tool for the studies of genome organization. At this stage, we have only visualized repetitive DNA elements. By adapting proper signal amplification strategies, single copy genes might become visible.

The use of exogenous proteins or RNPs to label endogenous DNA elements in live cells could potentially interfere with normal cellular functions. Indeed, it has been reported that the binding of LacI to the *lacO* repeats blocks DNA replication (Duxin et al., 2014). The use of TALE-lights in our experiments, however, didn't disrupt embryogenesis and was seemingly compatible with DNA replication (Yuan et al., 2014). Since TALE-lights can be used *in vitro* as a "sequence-specific DNA antibody", we examined fixed embryos and found that the appearance of histone marks on repetitive sequences was consistent with the dynamics scored in live embryos. This suggests that TALE-lights binding *in vivo* did not cause major disruptions. In addition, we noticed

that the majority of the TALE-light was displaced from the mitotic chromosomes, whereas the GFP-LacI stayed on (Holt et al., 2008). We reason that TALE-lights have a weaker DNA binding affinity, and thus are more tolerable by the cells. Nevertheless, the results generated by such a method should always be interpreted with caution, and it is important to point out that we did observe chromosome mis-segregation when a much higher concentration of the TALE-light was injected into the embryo.

Constitutive heterochromatin formation in development

The ability of the TALE-lights to discriminate individual satellite sequences has given us the capacity to reveal their differences in the establishment of constitutive heterochromatin during early embryogenesis. The 359-bp repeat recruits HP1a and becomes heterochromatinized in interphase 14, and it appears to typify one group of repeat sequences to which the initial recruitment of HP1a does not depend on the presence of H3K9me2/3. This group of repeat sequences was visualized as distinct loci of accumulation of the mutant HP1a (V26M) which is incapable of binding to H3K9me2/3 (Figure 4A). In contrast, the HP1a mutant with a deficient CSD (W200A) failed to localize to the 359-bp repeat but did localize to several foci in interphase 14 that appear to represent a second group of repeat sequences that recruit HP1a using an alternative mode of interaction, perhaps by chromodomain binding of H3K9me2/3 (Figure 4C). However, we have yet to identify a TALE-light marking this group of foci and additional work is needed to characterize the mode of HP1a recruitment to these sites. The third group of repetitive sequences includes 1.686 and *dodeca*. In terms of the classical hallmarks of heterochromatin, these repeats remain largely naïve at the time of the MBT. We do not know the molecular process of heterochromatin formation on these repeats. We suspect that the repeat-specific binding proteins, such as Prod for 1.686 (Torok et al., 2000) and DP1 for *dodeca* (Cortes and Azorin, 2000), could be involved. Another interesting possibility is that those repeats form heterochromatin via the spreading of the heterochromatic state from the adjacent satellite regions (e.g. the 359-bp region). Such "in trans" spreading of the heterochromatic state might be an important force shaping the chromatin landscape.

While we use the term heterochromatinization to describe the ensemble of changes associated with recruitment of HP1a to the 359-bp satellite, our findings suggest complexity in the processes that establish heterochromatin and some resulting ambiguity in terminology. HP1a and the histone modification that it associates with, H3K9me2/3, are often taken as markers that define heterochromatin. Even though this study provides direct evidence for the functional impact of a transition in chromatin structure marked by HP1a recruitment, the results also highlight the diversity in forms of heterochromatin. The satellite sequences have distinctive features prior to the recruitment of HP1a, including compaction and late replication in cycle 14 (Shermoen et al., 2010). Although the delay in replication of the 359-bp repeat prior to HP1a binding is slight, it is nonetheless delayed in cycle 14. Furthermore, the 1.686 satellite fails to mature to an HP1a-bound form until later in development, yet it maintains a compacted structure and late replication program. These observations reinforce a perspective that many factors influence the formation of "heterochromatin", and the degree of uniformity of the resulting chromatin structures remains to be established.

Controlling heterochromatinization in time and space at the MBT

The whole block of the 359-bp repeat undergoes heterochromatinization precisely in interphase 14. How does the embryo know when to form this heterochromatin? As mentioned earlier, fly embryos begin development with extremely fast nuclear divisions characterized by unusually high mitotic Cdk activity (Farrell and O'Farrell, 2014). Given that the binding of HP1a and its

silencing activity are both regulated by dynamic phosphorylation/dephosphorylation events (Zhao and Eissenberg, 1999; Zhao et al., 2001), the high kinase activity and the rapid cell divisions in the early embryo might curb the establishment of the stable heterochromatic state. Indeed, our results showed early accumulation of HP1a on the 359-bp repeat when Cdk1 activity was downregulated and the cell cycle arrested, suggesting that factors needed for heterochromatinization of the 359-bp repeat are already present in the early embryos and developmentally-regulated cell cycle slowing provides the first opportunity for their action (Figure 7G). However, recruitment of HP1a to foci of repeated sequences does not occur immediately in cycle 14, and the precise timing of this recruitment suggests sophisticated and as yet unknown regulatory circuitry.

Notably, constitutive heterochromatin is not always heterochromatic, at least according to the molecular hallmarks of this state. What marks the 359-bp sequences for selective formation of heterochromatin? It is notable that repeat sequences such as the 359-bp are selectively compacted during early mitotic cycles despite the absence of H3K9me2/3 (Shermoen et al., 2010), suggesting that some intrinsic feature of the satellite sequence might specify its special behavior. However, because only some of the constitutively heterochromatic repeats recruit HP1a, and there have been numerous findings suggesting maternal signals might act transgenerationally to direct aspects of gene activity, we sought to distinguish between a transacting maternal signal and sequence autonomous feature of the input.

Genetic manipulation of the amount of the 359-bp repeat in the mothers' genome (using either *D. simulans* or *D. melanogaster Zhr*^{1} mutant as mothers, see Figure 5) specifically influenced the heterochromatin formation on the 359-bp repeat in the offspring; whereas changes in the fathers' genome (the reciprocal crosses) had no such effect. These results suggest that maternal 359-bp sequence contribute to the zygotic establishment of heterochromatin at the 359-bp locus and encourage us to think of the type of signal that might be conveyed from mother to progeny. It has been established that particular RNAs expressed in the maternal germline are processed into a special class of small RNAs called piRNAs that act to silence gene expression. RNA homologous to the 359-bp repeat were found in the germinal tissues and the abundance of these transcripts was increased in mutants defective in components in the piRNA pathway suggesting that transcription of these sequences occurs and that the piRNA pathway targets this expression (Usakin et al., 2007). Current understanding of piRNA suppression of the expression of repeated sequences suggests that copies of the sequence in a specialized piRNA cluster in heterochromatic regions are expressed, processed and loaded onto an Argonaut protein called Piwi. Piwi in complex with a specific piRNA sequence appears capable of doing three things; directly targets homologous DNA sequences to promote heterochromatin formation and suppresses transcription, contributes to slicing activity that destroys the RNA products of homologous loci, and works in conjunction with other piRNA pathway components to amplify the piRNA signal by processing complementary and homologous RNA (Guzzardo et al., 2013). Piwi has been found to be associated with small RNAs derived from the 359-bp repeat region (Saito et al., 2006), consistent with a potential role of this pathway in regulating heterochromatin formation on these sequences. Our finding that HP1a is recruited to the 359-bp sequence at a specific time in cycle 14 and in a process that depends on the maternal presence of 359-bp sequences suggests that the 359-bp derived piRNAs are required for timely heterochromatinization of these sequences, although the details of the mechanism remain to be addressed.

Our finding that HP1 recruitment to the 359-bp sequences depends on a protein interaction domain that complexes with PxVxL motifs suggests a possible direct role of Piwi in recruiting HP1a. *Drosophila* HP1a and Piwi have been

shown to interact via the HP1a C-terminal binding domain with PxVxL-like motifs in Piwi (Brower-Toland et al., 2007; Mendez et al., 2011; Mendez et al., 2013). Recruitment by direct binding predicts localization of Piwi on the 359-bp sequences in amounts comparable to the HP1a that is recruited. However, we were unable to detect focal concentration of Piwi at the 359-bp repeat during the time of cycle 14 recruitment of HP1a. In fact, Piwi appeared rather diffused in the nucleus with only very slight localized signals (Figure S6B). These findings suggest that if Piwi complexes contribute to heterochromatinization of the 359-bp they act less directly, perhaps catalytically, or at an earlier time. We note that the 359-bp sequences fail to initiate replication at onset of cycle 14, and this small deferral in replication suggests that these sequences are distinguished from early replicating sequences prior to the recruitment of HP1a in cycle 14. We consequently suspect that the 359-bp sequences are somehow designated to be heterochromatic at an earlier time and that the signal that ultimately recruits HP1a is somewhat downstream of the initiating event.

Heterochromatin formation and timing of replication

We began with an interest in the developmental onset of late replication. We found that this onset is triggered by the down regulation of mitotic cyclin:Cdk1, which, if active during interphase, can trigger early replication of otherwise late replicating sequences (Farrell et al., 2012). While this finding indicates that a change in a "trans factor" acting on preexisting heterochromatin might be responsible for this onset, we found that heterochromatic marks were introduced at about the time of onset of late replication (Shermoen et al., 2010). Additionally, we noted that the onset of late replication is modulated differently at different repeat sequences (Yuan et al., 2014). These later observations suggest that changes of the chromatin structure of the repeat regions (cis-changes) also occur and might modulate replication timing.

Widespread coupling between heterochromatin and late replication have fostered the idea heterochromatin is late replicating. Additionally, the genomic context has been shown to influence the timing of firing of origins of replication, a finding that is generally interpreted as showing that local chromatin structure specifies replication timing. Nonetheless, despite strong connections, experimental support for a causal connection between heterochromatin and replication timing is indirect. Global knockdown of HP1a in *Drosophila* Kc cells by RNAi advanced the replication of centromeric repeats but delayed replication of many other genomic regions (Schwaiger et al., 2010). Such complex effects might be due to indirect effects of chromatin structure on overall genome arrangement (Sexton and Yaffe, 2015).

By manipulating HP1a level locally at specific repetitive loci, our results demonstrated that failure to establish a HP1a-bound state at the 359-bp repeat locus advanced its replication timing in cycle 15 and experimentally induced TALE-mediated HP1a recruitment to the 1.686 locus delayed its replication in cycle 15. This together with the natural developmental program of HP1a recruitment to the different satellite sequences strongly supports a causal connection between HP1a recruitment and replication-timing. It should be noted, however, that recruitment of HP1a can engage a number of reinforcing interactions among factors promoting heterochromatin formation. Hence, the results argue for a causal connection, but not necessarily a direct or even simple connection between HP1a recruitment and replication timing (Fig 7).

HP1a-positive regions unfold in conjunction with PCNA recruitment and replication, and with recruitment of repair proteins and repair of DNA damage (Chiolo et al., 2011; Shermoen et al., 2010). It is presently, unclear whether the events of repair and replication unfold the compacted heterochromatic structure, or whether a separate

decompaction process avails the compacted sequences to these reactions. However, in either case, compaction could impede these processes, and disassembly of the compacted structure might be regulatory. The activation and firing of replication origins involves complex assemblies regulated by several kinases and phosphatases. The dispersal of compacted heterochromatin might as well be regulated by the dynamic phosphorylation/dephosphorylation events and interplay between the structure and the activating processes might govern timing. Recent studies suggest that Rif1 is involved in specifying replication timing, perhaps via local recruitment of protein phosphatase 1 (Renard-Guillet et al., 2014). It will be interesting to test if this imbalance in the nuclear distribution of kinases and phosphatases has an impact on the organization of HP1a.

The development of genomic techniques such as Hi-C and DamID has revealed a modular organization of the genome. Topological domains, with the size spanning few tens of kilobases to several megabases, serve as functional units that make up the complex genome architecture (Cavalli and Misteli, 2013). The results shown in this study uncover clear distinctions between different repetitive sequences, and highlight the necessity of resolving constitutive heterochromatin into smaller sub-domains in future studies. We believe that a more modular view on heterochromatin will advance our understandings of its function, maintenance, and inheritance.

Experimental Procedures

TALE-lights assembly

Customized TALE arrays recognizing a given repetitive sequence were designed using the TAL Effector Nucleotide Targeter 2.0 (tale-nt.cac.cornell.edu). The following target sequences were chosen: 5'-AGC ACT GGT AAT TAG CTG CT-3' and 5'-AGC TGC TCA AAA CAG ATA TT-3' to target the 359-bp repeat; 5'-AGA ATA ACA TAG AAT AAC AT-3' to target the 1.686 repeat; 5'-CCC GTA CTG GTC CCG TAC T-3' to target the *dodeca* repeat.

The TALE arrays were assembled using the Golden Gate TALEN and TAL Effector Kit 2.0 (Addgene). Backbone plasmid MR015 was used in the final reaction. The full-length TALE array was then subcloned into the customized pET-28 bacterial expression vector carrying a C-terminal GFP or mCherry tag. These constructs were subsequently used to produce the recombinant TALE-light proteins.

Fly stocks

Drosophila strains were maintained on standard cornmeal-yeast medium. *D. melanogaster* strains used in this study were as follows: the *Sevelen* line as the wild type, *scute 8* (full genotype is $In(1)sc^{8},sc^{8}y^{31d}w^{a}$, Bloomington stock #798), Zhr^{1} (full genotype is *XYS.YL,Df(1)Zhr*, provided by Dr. Daniel Barbash). In the hybrid cross, 40-50 *D. simulans* virgins were mated to 50-60 *Sevelen* males in a confined vial for 2 days. Flies from several such vials were pooled into a population cage for embryo collection.

Protein production and microinjection

TALE-lights, as well as GFP-HP1a and GFP-PCNA, were produced in BL21 (DE3) competent *E.coli* cells (Bioline). Briefly, BL21 (DE3) transformants cultured in Luria-Bertani medium were treated with 0.5 mM IPTG to induce protein expression at room temperature for 12 hours. Bacteria were pelleted by centrifugation and resuspended in lysis buffer (20 mM Tris, pH 7.9, 500 mM NaCl, and 10 mM Imidazole). Then the bacteria were incubated on ice for 1 hour in the presence of 0.1 mg/ml lysozyme and 10 μM PMSF, and further lysed by sonication (ultrasonic liquid processors, Misonix). The recombinant protein in the cleared bacterial lysate was purified using Ni-NTA agarose (Macherey-Nagel). After thorough washes with wash buffer (20mM Tris, pH 7.9, 500 mM NaCl, and 20 mM Imidazole), the protein was eluted in elution buffer (20 mM Tris, pH 7.9, 200 mM NaCl, and 300 mM Imidazole), and then dialyzed into 40 mM Hepes, pH 7.4, and 150 mM KCl.

The microinjection was performed as previously described (Farrell et al., 2012). The TALE-lights were used at 1 μg/μl, GFP-HP1a at 6 μg/μl, and GFP-PCNA at 2 μg/μl. The fusion protein 1.686-HP1a was used at 0.1 μg/μl to induce ectopic HP1a recruitment (Figure 7).

Immunofluorescence and TALE-lights staining

Embryos were collected on grape-agar plates, dechorionated for 2 min in 50% bleach, and fixed in methanol-heptane (1:1) for 5 min. The fixed embryos were stored in methanol at -20°C. Before immune-staining, the embryos were first rehydrated gradually (5 min each in 1:3, 1:1, 3:1 PTA:methanol, then 10 min in PTA). PTA was PBS supplemented with 0.1% TritonX-100, and 0.02% Azide. The embryos were then blocked in PBTA (PTA plus 1% BSA) for 30 min, and incubated with primary antibodies (1:100 in PBTA) for 1 hour at room temperature or overnight at 4°C. The following primary antibodies were used: anti-Histone 3 (Abcam), anti-H3K9me3 (Millipore), anti-H3K9ac (Abcam), anti-H3K27ac (Abcam), anti-H3K27me3 (a gift

from Dr. Stavros Lomvardas), and anti-H4ac (pan-acetyl, a gift from Dr. Barbara Panning). The embryos were washed 3 times in PBTA (5 min each), and incubated with appropriate fluorescently labeled secondary antibodies (Molecular probes) for 1 hour in dark at room temperature. They were then washed 4 times in PBTA (5 min each), and mounted in Vectashield mounting medium with DAPI (Vector). For TALE-lights stainings, GFP or mCherry tagged purified TALE-lights protein (1:500) was included during the incubation with secondary antibodies.

Imaging, data quantification and interpretation

Embryos were imaged on a spinning-disk confocal microscope as previously described (Farrell et al., 2012), and the images were analyzed using Volocity 6 (Perkin Elmer). When imaging an individual repetitive sequence, the Z-scale was selected based on the TALE-light signals (usually 3-4 μm), and the step size in the Z-axis was 0.5 μm for fixed samples and 1 μm for live embryos. All the images in one experiment were acquired and processed using identical microscopic settings. In the TALE-lights staining experiments (Figure 2 and S2), a single optic section across the indicated repetitive loci was shown.

For the quantification of HP1a recruitment, optic sections containing the specific genomic loci were projected and corrected for photobleaching in Volocity. In each experiment, 3-7 embryos and 5-7 nuclei in each embryo were selected for quantification. In each nucleus, the mean intensity of GFP-HP1a at the TALE-light positive loci was divided by that at a control locus in that same nucleus to calculate the Fold Enrichment (Figure S3C). The mean and SD of those calculated Fold Enrichment in nuclei from different embryos were plotted against time, and then non-linear regression analysis was performed using Prism (GraphPad).

The results shown in this study were obtained with injected recombinant GFP-HP1a protein. We also performed the experiments with GFP-HP1a expressed from a transgene, and the results were identical. HP1a functions as a dimer, and thus a fraction of the injected GFP-HP1a mutant proteins could form hetero-dimer with the endogenous wild type HP1a. The possible existence of the hetero-dimer pool complicated the experimental scenario, but did not influence the interpretation on the contributions of different domains to the initial recruitment of HP1a.

Acknowledgements

We would like to express our gratitude to the members of the O'Farrell lab, especially Tony Shermoen and Hansong Ma, for continuous support and useful suggestions. We thank Geeta Narlikar, Blake Riggs, Barbara Panning, and Hiten Madhani for their comments on the manuscript, the UCSF ES Cell Targeting Core for constructing the TALE-lights, Zeid Rusan for analyzing the small RNA data, and Daniel Barbash, Hiroshi Kimura, Stavros Lomvardas, Barbara Panning, Patrick Ferree, Katalin Toth, Sarah Elgin, Haruhiko Siomi, William Theurkauf, William Sullivan for sharing reagents. This research was supported by the UCSF Program for Breakthrough Biomedical Research (to K.Y.), the UCSF CTSI-Strategic Opportunities Support Program (to K.Y.), and National Institutes of Health grant GM037193 (to P.H.O).

References

Anton, T., Bultmann, S., Leonhardt, H., and Markaki, Y. (2014). Visualization of specific DNA sequences in living mouse embryonic stem cells with a programmable fluorescent CRISPR/Cas system. Nucleus *5*, 163-172.

Beisel, C., and Paro, R. (2011). Silencing chromatin: comparing modes and mechanisms. Nature reviews. Genetics *12*, 123-135.

Blythe, S.A., and Wieschaus, E.F. (2015). Zygotic genome activation triggers the DNA replication checkpoint at the midblastula transition. Cell *160*, 1169-1181.

Brower-Toland, B., Findley, S.D., Jiang, L., Liu, L., Yin, H., Dus, M., Zhou, P., Elgin, S.C., and Lin, H. (2007). Drosophila PIWI associates with chromatin and interacts directly with HP1a. Genes Dev *21*, 2300-2311.

Canzio, D., Larson, A., and Narlikar, G.J. (2014). Mechanisms of functional promiscuity by HP1 proteins. Trends in cell biology *24*, 377-386.

Cavalli, G., and Misteli, T. (2013). Functional implications of genome topology. Nature structural & molecular biology *20*, 290-299.

Chen, B., Gilbert, L.A., Cimini, B.A., Schnitzbauer, J., Zhang, W., Li, G.W., Park, J., Blackburn, E.H., Weissman, J.S., Qi, L.S., *et al.* (2013). Dynamic imaging of genomic loci in living human cells by an optimized CRISPR/Cas system. Cell *155*, 1479-1491.

Chiolo, I., Minoda, A., Colmenares, S.U., Polyzos, A., Costes, S.V., and Karpen, G.H. (2011). Double-strand breaks in heterochromatin move outside of a dynamic HP1a domain to complete recombinational repair. Cell *144*, 732-744.

Chung, W.J., Okamura, K., Martin, R., and Lai, E.C. (2008). Endogenous RNA interference provides a somatic defense against Drosophila transposons. Current biology : CB *18*, 795-802.

Cortes, A., and Azorin, F. (2000). DDP1, a

heterochromatin-associated multi-KH-domain protein of Drosophila melanogaster, interacts specifically with centromeric satellite DNA sequences. Molecular and cellular biology *20*, 3860-3869.

Duxin, J.P., Dewar, J.M., Yardimci, H., and Walter, J.C. (2014). Repair of a DNA-protein crosslink by replication-coupled proteolysis. Cell *159*, 346-357.

Edgar, B.A., and O'Farrell, P.H. (1990). The three postblastoderm cell cycles of Drosophila embryogenesis are regulated in G2 by string. Cell *62*, 469-480.

Elgin, S.C., and Reuter, G. (2013). Position-effect variegation, heterochromatin formation, and gene silencing in Drosophila. Cold Spring Harbor perspectives in biology *5*, a017780.

Fadloun, A., Eid, A., and Torres-Padilla, M.E. (2013). Mechanisms and dynamics of heterochromatin formation during mammalian development: closed paths and open questions. Current topics in developmental biology *104*, 1-45.

Farrell, J.A., and O'Farrell, P.H. (2014). From egg to gastrula: how the cell cycle is remodeled during the Drosophila mid-blastula transition. Annual review of genetics *48*, 269-294.

Farrell, J.A., Shermoen, A.W., Yuan, K., and O'Farrell, P.H. (2012). Embryonic onset of late replication requires Cdc25 down-regulation. Genes & Development *26*, 714-725.

Ferree, P.M., and Barbash, D.A. (2009). Species-specific heterochromatin prevents mitotic chromosome segregation to cause hybrid lethality in Drosophila. PLoS biology *7*, e1000234.

Gu, T., and Elgin, S.C. (2013). Maternal depletion of Piwi, a component of the RNAi system, impacts heterochromatin formation in Drosophila. PLoS genetics *9*, e1003780.

Guzzardo, P.M., Muerdter, F., and Hannon, G.J. (2013). The piRNA pathway in flies: highlights and future directions. Current opinion in genetics & development *23*, 44-52.

Hathaway, N.A., Bell, O., Hodges, C., Miller, E.L., Neel, D.S., and Crabtree, G.R. (2012). Dynamics and memory of heterochromatin in living cells. Cell *149*, 1447-1460.

He, B., Caudy, A., Parsons, L., Rosebrock, A., Pane, A., Raj, S., and Wieschaus, E. (2012). Mapping the pericentric heterochromatin by comparative genomic hybridization analysis and chromosome deletions in Drosophila melanogaster. Genome research *22*, 2507-2519.

Holt, L.J., Krutchinsky, A.N., and Morgan, D.O. (2008). Positive feedback sharpens the anaphase switch. Nature *454*, 353-357.

Jachowicz, J.W., Santenard, A., Bender, A., Muller, J., and Torres-Padilla, M.E. (2013). Heterochromatin establishment at pericentromeres depends on nuclear position. Genes Dev *27*, 2427-2432.

Krassovsky, K., and Henikoff, S. (2014). Distinct chromatin features characterize different classes of repeat sequences in Drosophila melanogaster. BMC genomics *15*, 105.

Lee, M.T., Bonneau, A.R., and Giraldez, A.J. (2014). Zygotic genome activation during the maternal-to-zygotic transition. Annual review of cell and developmental biology *30*, 581-613.

Levinger, L., and Varshavsky, A. (1982). Protein D1 preferentially binds A + T-rich DNA in vitro and is a component of Drosophila melanogaster nucleosomes containing A + T-rich satellite DNA. Proceedings of the National Academy of Sciences of the United States of America *79*, 7152-7156.

Levsky, J.M., and Singer, R.H. (2003). Fluorescence in situ hybridization: past, present and future. Journal of cell science *116*, 2833-2838.

Li, X.Y., Harrison, M.M., Villalta, J.E., Kaplan, T., and Eisen, M.B. (2014). Establishment of regions of genomic activity during the Drosophila maternal to zygotic transition. eLife *3*.

Lindhout, B.I., Fransz, P., Tessadori, F., Meckel, T., Hooykaas, P.J., and van der Zaal, B.J. (2007). Live cell imaging of repetitive DNA sequences via GFP-tagged polydactyl zinc finger proteins. Nucleic acids research *35*, e107.

Lu, B.Y., Ma, J., and Eissenberg, J.C. (1998). Developmental regulation of heterochromatin-mediated gene silencing in Drosophila. Development *125*, 2223-2234.

Ma, H., Reyes-Gutierrez, P., and Pederson, T. (2013). Visualization of repetitive DNA sequences in human chromosomes with transcription activator-like effectors. Proceedings of the National Academy of Sciences of the United States of America *110*, 21048-21053.

Mendez, D.L., Kim, D., Chruszcz, M., Stephens, G.E., Minor, W., Khorasanizadeh, S., and Elgin, S.C. (2011). The HP1a disordered C terminus and chromo shadow domain cooperate to select target peptide partners. Chembiochem : a European journal of chemical biology *12*, 1084-1096.

Mendez, D.L., Mandt, R.E., and Elgin, S.C. (2013). Heterochromatin Protein 1a (HP1a) partner specificity is determined by critical amino acids in the chromo shadow domain and C-terminal extension. The Journal of biological chemistry *288*, 22315-22323.

Miyanari, Y., Ziegler-Birling, C., and Torres-Padilla, M.E. (2013). Live visualization of chromatin dynamics with fluorescent TALEs. Nature structural & molecular biology *20*, 1321-1324.

Padeken, J., and Heun, P. (2014). Nucleolus and nuclear periphery: Velcro for heterochromatin. Current opinion in cell biology *28C*, 54-60.

Renard-Guillet, C., Kanoh, Y., Shirahige, K., and Masai, H. (2014). Temporal and spatial regulation of eukaryotic

DNA replication: from regulated initiation to genome-scale timing program. Semin Cell Dev Biol *30*, 110-120.

Robinett, C.C., Straight, A., Li, G., Willhelm, C., Sudlow, G., Murray, A., and Belmont, A.S. (1996). In vivo localization of DNA sequences and visualization of large-scale chromatin organization using lac operator/repressor recognition. The Journal of cell biology *135*, 1685-1700.

Rudolph, T., Yonezawa, M., Lein, S., Heidrich, K., Kubicek, S., Schafer, C., Phalke, S., Walther, M., Schmidt, A., Jenuwein, T., *et al.* (2007). Heterochromatin formation in Drosophila is initiated through active removal of H3K4 methylation by the LSD1 homolog SU(VAR)3-3. Molecular cell *26*, 103-115.

Saito, K., Nishida, K.M., Mori, T., Kawamura, Y., Miyoshi, K., Nagami, T., Siomi, H., and Siomi, M.C. (2006). Specific association of Piwi with rasiRNAs derived from retrotransposon and heterochromatic regions in the Drosophila genome. Genes Dev *20*, 2214-2222.

Schwaiger, M., Kohler, H., Oakeley, E.J., Stadler, M.B., and Schubeler, D. (2010). Heterochromatin protein 1 (HP1) modulates replication timing of the Drosophila genome. Genome research *20*, 771-780.

Segal, D.J., Dreier, B., Beerli, R.R., and Barbas, C.F., 3rd (1999). Toward controlling gene expression at will: selection and design of zinc finger domains recognizing each of the 5'-GNN-3' DNA target sequences. Proceedings of the National Academy of Sciences of the United States of America *96*, 2758-2763.

Sexton, T., and Yaffe, E. (2015). Chromosome folding: driver or passenger of epigenetic state? Cold Spring Harbor perspectives in biology *7*, a018721.

Shermoen, A.W., McCleland, M.L., and O'Farrell, P.H. (2010). Developmental control of late replication and S phase length. Current biology : CB *20*, 2067-2077.

Simon, J.A., and Kingston, R.E. (2013). Occupying chromatin: Polycomb mechanisms for getting to genomic targets, stopping transcriptional traffic, and staying put. Molecular cell *49*, 808-824.

Stasevich, T.J., Hayashi-Takanaka, Y., Sato, Y., Maehara, K., Ohkawa, Y., Sakata-Sogawa, K., Tokunaga, M., Nagase, T., Nozaki, N., McNally, J.G., *et al.* (2014). Regulation of RNA polymerase II activation by histone acetylation in single living cells. Nature *516*, 272-275.

Thanisch, K., Schneider, K., Morbitzer, R., Solovei, I., Lahaye, T., Bultmann, S., and Leonhardt, H. (2014). Targeting and tracing of specific DNA sequences with dTALEs in living cells. Nucleic acids research *42*, e38.

Torok, T., Gorjanacz, M., Bryant, P.J., and Kiss, I. (2000). Prod is a novel DNA-binding protein that binds to the 1.686 g/cm(3) 10 bp satellite repeat of Drosophila melanogaster. Nucleic acids research *28*, 3551-3557.

Usakin, L., Abad, J., Vagin, V.V., de Pablos, B., Villasante, A., and Gvozdev, V.A. (2007). Transcription of the 1.688 satellite DNA family is under the control of RNA interference machinery in Drosophila melanogaster ovaries. Genetics *176*, 1343-1349.

Vlassova, I.E., Graphodatsky, A.S., Belyaeva, E.S., and Zhimulev, I.F. (1991). Constitutive heterochromatin in early embryogenesis of Drosophila melanogaster. Molecular & general genetics : MGG *229*, 316-318.

Waters, J.C. (2009). Accuracy and precision in quantitative fluorescence microscopy. The Journal of cell biology *185*, 1135-1148.

Wei, K.H., Grenier, J.K., Barbash, D.A., and Clark, A.G. (2014). Correlated variation and population differentiation in satellite DNA abundance among lines of Drosophila melanogaster. Proceedings of the National Academy of Sciences of the United States of America *111*, 18793-18798.

Yuan, K., Shermoen, A.W., and O'Farrell, P.H. (2014). Illuminating DNA replication during Drosophila development using TALE-lights. Current biology : CB *24*, R144-145.

Zemach, A., McDaniel, I.E., Silva, P., and Zilberman, D. (2010). Genome-wide evolutionary analysis of eukaryotic DNA methylation. Science *328*, 916-919.

Zhao, T., and Eissenberg, J.C. (1999). Phosphorylation of heterochromatin protein 1 by casein kinase II is required for efficient heterochromatin binding in Drosophila. The Journal of biological chemistry *274*, 15095-15100.

Zhao, T., Heyduk, T., and Eissenberg, J.C. (2001). Phosphorylation site mutations in heterochromatin protein 1 (HP1) reduce or eliminate silencing activity. The Journal of biological chemistry *276*, 9512-9518.